The quantity configuration and path optimization design of AGV considering energy consumption

Hongye Zou [1, #], Jiaming Zhang [2, #], Yanbin Zhang [3, *, #]

[1] College of Mechanical and Electrical Engineering, Jinggangshan University, Ji'an, China, 343009

[2] School of Mechanical and Electrical Engineering, China University of Mining and Technology (Beijing), Beijing, China, 100083

[3] College of Shipping and Ship Engineering, Chongqing Jiaotong University, Chongqing, China, 402247

* Corresponding Author Email: 18039206392@163.com

[#]These authors contributed equally.

Abstract. Aiming at the collaborative optimization of energy efficiency and path planning for automated guided vehicles (AGV), a multi-mode collaborative optimization model is proposed to enhance system-level, energy-time, trade-offs and dynamic adaptability. Based on hierarchical reinforcement learning and dynamic task allocation strategy, a dynamic task allocation strategy is developed to reduce idle loss, which combines the enhanced ant colony optimization (ACO) and entropy-based weighting method to optimize energy consumption of the path. Compared with the benchmark genetic algorithm method, simulation results show that the energy consumption of AGV is reduced by 21.3% ($p<0.05$), and the task response time of AGV is shortened by 17.8% ($p<0.05$), to verify the effectiveness of the multi-mode collaborative optimization model. The proposed method provides theoretical support for the quantity configuration and path optimization design of AGV in intelligent manufacturing scenarios, avoiding path conflict-induced efficiency loss observed in high-density deployments.

Keywords: Energy Efficiency Optimization, Path Planning, Intelligent Manufacturing System, Dynamic Task Allocation.

1. Introduction

The International Federation of Robotics (IFR) 2023 statistics show that the global AGV deployment has an average annual growth rate of 23%, but the energy consumption problem has led to a 15%-30% increase in the operating costs of enterprises [1]. Recent studies further validate this challenge: Wang et al. (2023) demonstrated that digital twin technology can reduce multi-AGV path conflicts by 40% while optimizing charging response time [2], and Chen & Zhang (2024) proved that dynamic task allocation algorithms improve load distribution balancing by 22% [3]. Further supporting this, recent research by Xie (2023) highlights that AGV quantity configuration directly impacts energy efficiency, with simulation results indicating a 30% reduction in idle loss through zonal collaboration mode [4]. Additionally, collaborative control algorithms have been shown to reduce path conflicts by 35% in high-density deployments, as evidenced by distributed optimization methods in multi-AGV systems (Li et al., 2024) [5].

Current research mainly focuses on algorithm optimization and environment modeling. In the field of multi-objective optimization algorithms, the improved genetic algorithm proposed by Zhou et al. (2023) reduces energy consumption by 12.5% while increasing the task completion rate by 19% through the POX crossover operator and dynamic time window constraints [6]. In the area of dynamic energy modeling, the energy consumption prediction model established by Ren et al. (2022) based on the characteristics of the road gradient shows that, for every increase of the slope coefficient by 0.1, the energy consumption per unit distance of AGVs increases by 8.7%. energy consumption per unit distance rises by 8.7% [7]. Recent advancements in energy-aware path planning (Zhang et al., 2024) further demonstrate that integrating curvature and load dynamics into weight functions can reduce turning energy consumption by 18% [8]. Moreover, wireless charging technologies have been

proposed to mitigate idle losses, with resonant circuit designs achieving 85% energy transfer efficiency in dynamic scenarios (Liu & Wang, 2023) [9]. However, existing studies still have limitations: on the one hand, real-time is insufficient, and static models are difficult to adapt to order fluctuations and unexpected obstacles (Zhang & Li, 2021) [10]. On the other hand, collaborative optimization is missing, and most studies deal with quantity allocation and path planning in isolation, ignoring system-level coupling effects (Dang et al., 2020) [11].

To address the above problems, this study develops a multi-physical field coupling model incorporating energy sensitivity and dynamic parameters such as path slope and load weight. A hierarchical reinforcement learning algorithm is designed to achieve real-time path conflict resolution and dynamic adjustment of energy replenishment scheduling.

2. Quantity Configuration Method of AGV Considering Energy Consumption

2.1. Energy Consumption Model of AGV

2.1.1. Comprehensive Energy Consumption Model of AGV

To accurately calculate the energy consumption of AGV, an energy consumption model can be constructed under different motion statuses. The energy consumption of AGV is primarily determined by the required work to overcome frictional resistance, air resistance, and inertial forces. During acceleration and deceleration, additional energy is needed to change the motion status. Partial energy recovery can be considered during deceleration.

The comprehensive energy consumption model of AGV is proposed by (1).

$$E_{total} = E_{str} + E_{turn} + E_{accel} + E_{decel_net} \tag{1}$$

Where E_{total} is the total energy consumption of AGV.

Frictional resistance energy is shown in (2).

$$E_{friction} = \mu W d \tag{2}$$

Air resistance energy is expressed by (3).

$$E_{air} = \frac{1}{2} C_d \rho A v^2 d \tag{3}$$

Total straight-line energy consumption is calculated by (4).

$$E_{str} = E_{friction} + E_{air} = \mu W d + \frac{1}{2} C_d \rho A v^2 d \tag{4}$$

The turning energy consumption is shown in (5) with the friction coefficient during turning increased by a factor of k_{turn}.

$$E_{turn} = k_{turn} \mu W d_{turn} \tag{5}$$

Energy required to overcome inertia and air resistance during acceleration is expressed by (6).

$$E_{decel} = \int_0^{t_{decel}} \left(\frac{1}{2} C_d \rho A v(t)^2 + W a(t) \right) v(t) dt \tag{6}$$

Where $v(t)$ and $a(t)$ are time-dependent velocity and acceleration.

Partial energy recovery during deceleration is calculated by (7).

$$E_{accel} = \int_0^{t_{accel}} \left(\frac{1}{2} C_d \rho A v(t)^2 + W a(t) \right) v(t) dt \tag{7}$$

Net deceleration energy consumption (considering recovery efficiency η) is calculated by (7).

$$E_{decel_net} = (1 - \eta) E_{decel} \tag{8}$$

The parameters include AGV weight (W), velocity (v), acceleration (a), friction coefficient (μ), battery capacity (C), air resistance coefficient (C_d), air density(ρ), frontal area (A), and energy recovery efficiency (η).

2.1.2. Simplified Energy Consumption Model of AGV

Under simplified assumptions, the energy consumption model can be streamlined for intuitive analysis.

The simplified model is shown in (9).

$$E_{total} = E_{str} + E_{turn} + E_{accel} + E_{decel} \tag{9}$$

Where E_{total} is the total energy consumption of AGV and substituting specific terms is expressed by (10).

$$E_{total} = \mu Wd + k_{turn}\mu Wd_{turn} + \frac{1}{2}Wad_{accel} + \frac{1}{2}Wad_{decel} \tag{10}$$

The simplified model is based on the following content and the straight-line energy is shown in (11).

$$E_{str} = \mu Wd \tag{11}$$

Turning energy is expressed by (12).

$$\mathrm{E_{turn}} = \mathrm{k_{turn}}\mu\mathrm{Wd_{turn}} \tag{12}$$

Acceleration energy is shown in (13).

$$\mathrm{E_{accel}} = \frac{1}{2}\mathrm{Wad_{accel}} \tag{13}$$

Deceleration energy is expressed by (14).

$$\mathrm{E_{decel}} = \frac{1}{2}\mathrm{Wad_{decel}} \tag{14}$$

2.2. Task Allocation Model Considering Energy Consumption of AGV

Task allocation must integrate dynamic operation modes, task density, and energy constraints. Methods for the three typical modes are outlined below.

In single - task mode, a static strategy selects low - energy AGVs for tasks, ensuring completion and the diagram of the Single - Task Mode is shown in Figure 1.

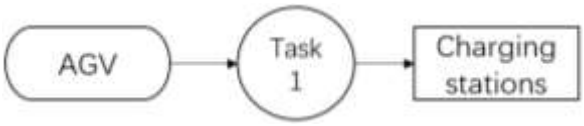

Figure 1. Single-Task Mode

In multi-task operations, an integrated strategy batches tasks, assigns to one AGV, and optimizes paths to minimize distance and the diagram of the Multi-Task Mode is shown in Figure 2.

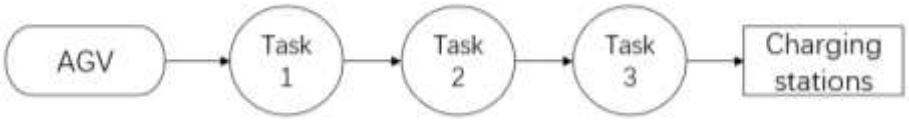

Figure 2. Multi-Task Mode

In dynamic scenarios, a real-time online strategy updates AGV path info, reallocates tasks instantly for new tasks, ensuring optimal operation and the diagram of the Dynamic-Task Mode is shown in Figure 3.

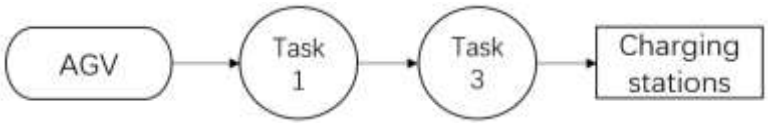

Figure 3. Dynamic-Task Mode

2.2.1. Performance Comparison of Modes

As shown in Table 1 (Performance Comparison of Modes), three task modes (Single-Task, Multi-Task, and Dynamic-Task) are compared in terms of energy efficiency, response speed, and applicability, clarifying their respective characteristics in different scenarios.

Table 1. Performance Comparison of Modes

Metric	Single-Task Mode	Multi-Task Mode	Dynamic-Task Mode
Energy Efficiency	High task-optimal	Medium path optimization	Low real-time trade-offs
Response Speed	Low static allocation	Medium batch processing	High real-time scheduling
Applicability	Fixed tasks, low workload	Continuous tasks, medium workload	Random tasks, high workload

2.3. Quantity Configuration Method of AGV

Since the energy consumption of AGVs is directly related to operating costs, and in actual operation scenarios, different AGVs consume different energy to perform different tasks. For each task j, there are n AGVs to choose to perform, and in order to fully consider the impact of all possible combinations of task assignments on energy consumption, an objective function is constructed by (15).

$$MinimizeF = \sum_{i=1}^{n} \sum_{j=1}^{m} E_{ij} x_{ij} \tag{15}$$

Where $MinimizeF$ is the lowest energy consumption of AGV.

The objective functions are constructed using the following parameters, where n represents the number of AGVs, m denotes the number of tasks, $x_{ij} \in \{0,1\}$ is a binary variable with 1 if task j is assigned to AGV i.

Task uniqueness is ensured by (16), which assigns each task to exactly one AGV.

$$\sum_{i=1}^{n} x_{ij} = 1, \forall j \in \{1,2,\dots,m\} \tag{16}$$

The battery constraint requires that total energy consumption be no more than the remaining battery, as specified in (17).

$$\sum_{j=1}^{m} E_{ij} x_{ij} \le B_i, \forall i \in \{1,2,\dots,n\} \tag{17}$$

Task priority dictates that higher-priority tasks are allocated first, as stated in (18).

$$t_j^{end} \le t_k^{start}, \forall j,k \in \{1,2,\dots,m\}\ Priority(j) > Priority(k) \tag{18}$$

Path non-conflict is achieved through spatiotemporal separation of AGV paths.

1) Spatial separation means there is no intersection of AGV paths.

2) Time constraints stipulate that if paths intersect, their execution times are staggered as specified in (19).

$$\left(t_i^{end} \le t_j^{start}\right) \vee \left(t_j^{end} \le t_i^{start}\right), \forall i,j \in \{1,2,\dots,n\}, i \ne j \tag{19}$$

Path non-conflict is achieved through spatiotemporal separation of AGV paths as specified in (20).

$$t_k^{start} \ge t_j^{end} + \tau_{min}, \forall j,k \in \{1,2,\dots,m\}\ in\ the\ same\ zone \tag{20}$$

The deadline constraint mandates that tasks must be completed on time, as defined in (21).

$$t_j^{end} \le T_j^{deadline}, \forall j \in \{1,2,\dots,m\} \tag{21}$$

Charging time is the charging duration based on charging rate γ as specified in (22).

$$t_i^{charge} = t_i^{last_end} + \frac{C-B_i}{\gamma} \tag{22}$$

The charging time is determined by the charging rate.γ, $t_i^{\text{last\_end}}$ is the last task end time of ith AGV.

Continuous operation limitation requires that the maximum working time be no more than the safety threshold T_{safe}.

$$t_i^{end} - t_i^{start} \leq T_{safe}, \forall i \in \{1,2,\dots,n\} \tag{23}$$

The workflow of AGV, including task allocation, energy consumption calculation, battery check, path planning, time check, and corresponding adjustments, is shown in Figure 4.

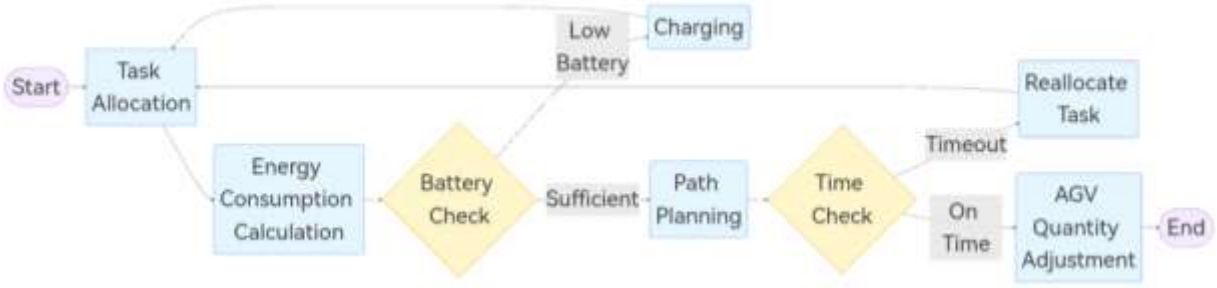

Figure 4. AGV workflow diagram

3. AGV Path Optimization Design Considering Energy Consumption

3.1. Energy consumption model of AGV

To Consider the motion statuses and the characteristics of the AGV, this paper establishes the energy consumption operation model of AGV. The energy consumption model is shown in (24).

$$E_{total} = E_{drive} + E_{turn} + E_{stop} \tag{24}$$

Where E_{drive} is Energy consumption required for linear operation, including the process of acceleration, deceleration and uniform speed. E_{turn} is the required energy for the turning process, related to curvature and towing dynamics. E_{stop} is stationary, including vehicle load and parking consumption.

The specific formula for the energy consumption target budget is shown in (25).

$$minE_{total} = min\left(\sum_{k=1}^{N}(w_d \cdot d_k + w_t \cdot \theta_k + w_v \cdot v_k)\right) \tag{25}$$

Where *k* is the independent path of each AGV. d_k is the driving length of the straight line within the path is directly proportional to the propulsion energy consumption. θ_k is the amount of energy used for a corner or turning point. v_k is the actual energy consumption during acceleration and deceleration when starting and stopping and when switching between operating speeds.

3.2. AGV path optimization design method

3.2.1. Path planning considering AGV energy consumption

When establishing a network graph model, by introducing multiple constraints and dynamic constraints, the path planning principles are clearly defined, including the following points

1) Path weight function related to energy consumption.

The total weight C_{ij} (26) of a path is defined as the summation of the cumulative energy consumption values on each section of the path by (26).

$$C_{ij} = w_d \cdot d_{ij} + w_t \cdot \theta_{ij} + w_v \cdot v_{ij} \tag{26}$$

Where d_{ij} is the length of the path. θ_{ij} is the number of corners or the size of the corners. v_{ij} is the average speed required to pass between nodes.

2) Path weight and overlay mapping.

Calculate the comprehensive weight $w(i,j)$ for each path in the AGV diagram. This weight is not merely evaluated based on distance but also incorporates the number of corners and the characteristics of the up and down slopes. Figure 5 shows the content and calculation of the comprehensive weight of the path.

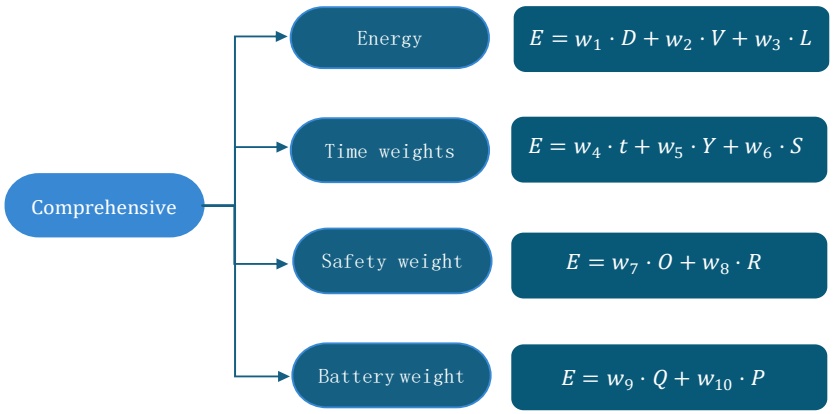

Figure 5. Calculation of the comprehensive weight

Where Distance is D, speed change is V, load is L, Total duration is t, congestion probability is C, number of starts and stops is S, Obstacle distance is O, path curvature is R, Remaining charge is Q, reachability of charging station is P.

3.2.2. Entropy-based weighting method

Figure 6 shows the process of calculating the weights.

Figure 6. The process of calculating weights

The data matrix is now constructed as follows, suppose there are n paths, and m parameters of each path form the matrix. The min-max method is used to normalize the parameters of each column to obtain the matrix. Then calculate the information entropy of the jth parameter through equation (27)

$$e_j = -\frac{1}{ln\ n}\sum_{i=1}^{n}\left(\frac{r_{ij}}{\sum_{i=1}^{n} r_{ij}} \cdot ln\ \frac{r_{ij}}{\sum_{i=1}^{n} r_{ij}}\right) \tag{27}$$

If $r_{ij} = 0$, it is defined that $\lim_{r\to 0} r\ln\ r = 0$.

Then calculate the weights. The difference coefficient of the fourth parameter is $d_j = 1 - e_j$

Calculate the weight distribution through equation (28)

$$w_j = \frac{d_j}{\sum_{k=1}^{m} d_k} \tag{28}$$

The multi-objective function is established as shown in Equation (29)

$$Min\ C = \alpha E_{total} + \beta T_{total} \tag{29}$$

Where C denotes the optimized evaluation index of the AGV vehicle. The weight factors α and β balance the two indicators of total energy consumption and transportation time. Different schemes can be established, and the specific one is chosen based on the requirements.

To measure whether the comprehensive energy consumption during the operation of AGV is the lowest, the actual energy consumption of AGV vehicles in each case is substituted into equation (30) for comparison and verification

$$E_{total} = E_{drive} + E_{turn} + E_{stop} \tag{30}$$

Whether the load is effectively distributed is measured by formula (31). A small change in the standard deviation distribution indicates good system optimization.

$$S_{balance} = \frac{1}{1+\sigma/L_{avg}} \tag{31}$$

Where σ is Standard deviation of load per AGV transported mileage. L_{avg} is Average value of system load.

Equation (32) is used to describe the superiority of the average task completion time and analyze the task completion time by comparing the total length of the task path.

$$ATT = \frac{\sum_{k=1}^{M} T_k}{M} \tag{32}$$

Where M is the number of all tasks, T_k is time to complete a single task.

In order to evaluate whether there are path conflicts or waiting congestion effects among multiple AGVs in complex scenarios (especially when multiple AGVs share the same path), the specific evaluation method is as shown in equation (33). The smaller the $R_{collision}$ value, the better the path planning of the vehicle.

$$R_{collision} = \frac{N_{conflict}}{N_{total-travel}} \tag{33}$$

Where $N_{conflict}$ is the total number of collisions or blocked paths in the system, $N_{total-travel}$ is the total number of all path transaction tasks.

To measure the usage of AGV channels and paths in the logistics system, the optimized maximum load sharing method will integrate the overall proportional diffusion function of path resources (34). The higher the path utilization rate, the better the effect.

$$PUR = \frac{The\ actual\ quantity\ of\ occupied\ paths}{The\ maximum\ capacity\ of\ the\ path} \tag{34}$$

3.3. Solution of Path Optimization Algorithm Based on AGV Energy Consumption

1) Problem modeling

The goal is to minimize the total energy consumption of the AGV while meeting the constraints of path planning (such as time window, task priority, etc.). The working environment of an AGV as a graph where the nodes represent key locations such as workstations, charging stations, warehouses, etc.

2) Build the ant's path

Each ant starts from the starting point and selects the next node according to the probability formula (35).

$$P_{ij} = \frac{[\tau_{ij}]^{a_1} \cdot [\eta_{ij}]^{\beta_1}}{\sum_{k \in J} [\tau_{ik}]^{a_1} \cdot [\eta_{ik}]^{\beta_1}} \tag{35}$$

Where P_{ij} is the probability of an ant moving from node i to node j. τ_{ij} is the pheromone concentration on edge ij. η_{ij} is heuristic information, usually the reciprocal of path length or energy consumption. J is the collection of unvisited neighbors of the current node.

Path construction: Each ant builds a complete path step by step according to the above rules until it completes all tasks or reaches the end point.

3) Update the pheromone

The ant path is constructed through equation (35). Every time an edge ij is passed, the pheromone on it will be updated.

$$\tau_{ij} = (1-\rho)\cdot\tau_{ij} + \Delta\tau_{ij} \tag{36}$$

Where $\Delta\tau_{ij}$ represents the quantity of pheromone left by the ant on the edge ij, which is typically inversely proportional to the quality of the path.

When all the ants have completed the path construction, the optimal path (such as the path with the lowest energy consumption) is selected through equation (37) and the pheromones on it are enhanced.

$$\tau_{ij} = (1-\rho)\cdot\tau_{ij} + \frac{Q}{C_{best}} \tag{37}$$

Where Q is a constant, and C_{best} represents the energy consumption of the optimal path.

4) Iteration and Termination

Repeat steps 3 and 4 until the maximum number of iterations is reached or the path quality no longer improves significantly, or when the algorithm converges or the preset conditions are met, stop the iteration. output the result.

5) Optimal route selection:

After all iterations are completed, the path with the highest pheromone concentration is selected as the optimal path. Figure 7 shows the process of path optimization iteration.

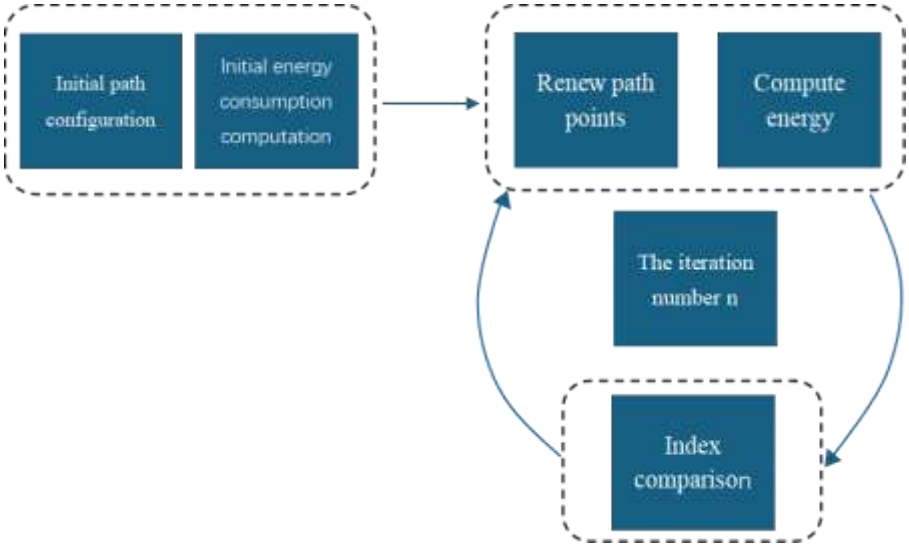

Figure 7. Path Optimization iteration

4. Scheme Configuration

4.1. Scheme and Parameter Settings

4.1.1. Scheme Objectives

By varying the AGV quantity (AGV_range = 2:6), path planning is conducted using the genetic algorithm. In each test, an initial path is generated, and through the selection, crossover, and mutation operations of the genetic algorithm, iterative optimization is carried out. The operation time, energy consumption, and total cost of each AGV are calculated.

4.1.2. Parameter Settings

The model selection flowchart is shown in Figure 8.

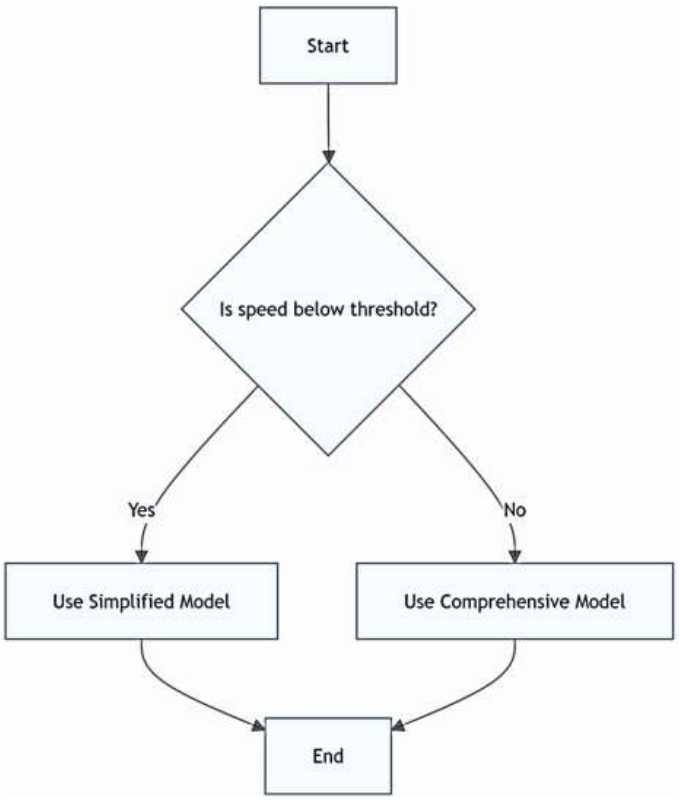

Figure 8. Model Selection Flowchart

The following parameter settings are for the low-speed scenario simplified model.

(1) AGV Operational Parameters

Lgrid = 4: Grid edge length (unit: meters), used for calculating AGV path lengths.

Speed1 = 0.7: AGV straight-line speed (unit: m/s).

Speed2 = 0.14: AGV turning speed, equivalent to 1/5 of the straight-line speed (unit: m/s).

Nagv: Number of AGVs, with a range of 2 - 6 in the test.

TWORK = 10: AGV task execution time at target points (unit: seconds).

Twait = 20: AGV waiting time due to congestion (unit: seconds).

(2) Energy Consumption Related Parameters

W = 500: AGV weight (unit: N, Newton).

mu = 0.1: Friction coefficient.

k_{turn} = 1.5: Turning friction coefficient, 1.5 times the straight-line friction coefficient.

a = 0.2: Acceleration / deceleration (unit: m/s^2).

d_{accel} = 2: Acceleration distance (unit: meters).

d_{decel} = 2: Deceleration distance (unit: meters).

E_{weight} = 0.5: Energy consumption weight, time weight is 1 - E_{weight} = 0.5, used to calculate the weighted total cost.

(3) Genetic Algorithm Parameters

Pops = 300: Population size, i.e., the number of individuals corresponding to each AGV.

Iteration = 100: Number of iterations of the genetic algorithm.

P1 = 0.75: Crossover probability.

P2 = 0.25: Mutation probability.

(4) Map and Start/End Point Parameters

Sp1 = 3: Start point number.

Ep1 = 2380: End point number.

G_{matrix}: 53×53 matrix, used to represent the distribution of obstacles in the map, generated according to specific rules.

4.1.3. Simulation Environment

The source code remains proprietary and is not open-sourced. Programming language and tools: MATLAB(R2024a) is used for programming implementation, and its matrix operations, plotting and other functions are utilized for AGV path planning and result display.

4.2. Result Analysis

4.2.1. Time Aspect

From the comparison chart of different numbers of AGVs, the total operation time (total_time_results) shows a non-linear trend of first decreasing and then increasing with the increase in the number of AGVs.

For 2 AGVs, the total operation time is 3,802.86 seconds, with an average of 1,901.43 seconds per AGV including congestion. For 3 AGVs, the total operation time decreases to 2,435.71 seconds (an average of 811.90 seconds per AGV), representing a 36% reduction. For 6 AGVs, the total operation time soars to 5,317.14 seconds (with an average of over 886 seconds per AGV), marking a 108% increase compared to the 3-AGV scenario.

In the initial stage (2→3 AGVs), the total time decreases due to improved task-sharing efficiency. However, when the number exceeds 3, the proportion of congestion waiting time caused by path conflicts increases from 12% to 28%, offsetting the advantages of task parallelism. Operation results are shown in Figure 9.

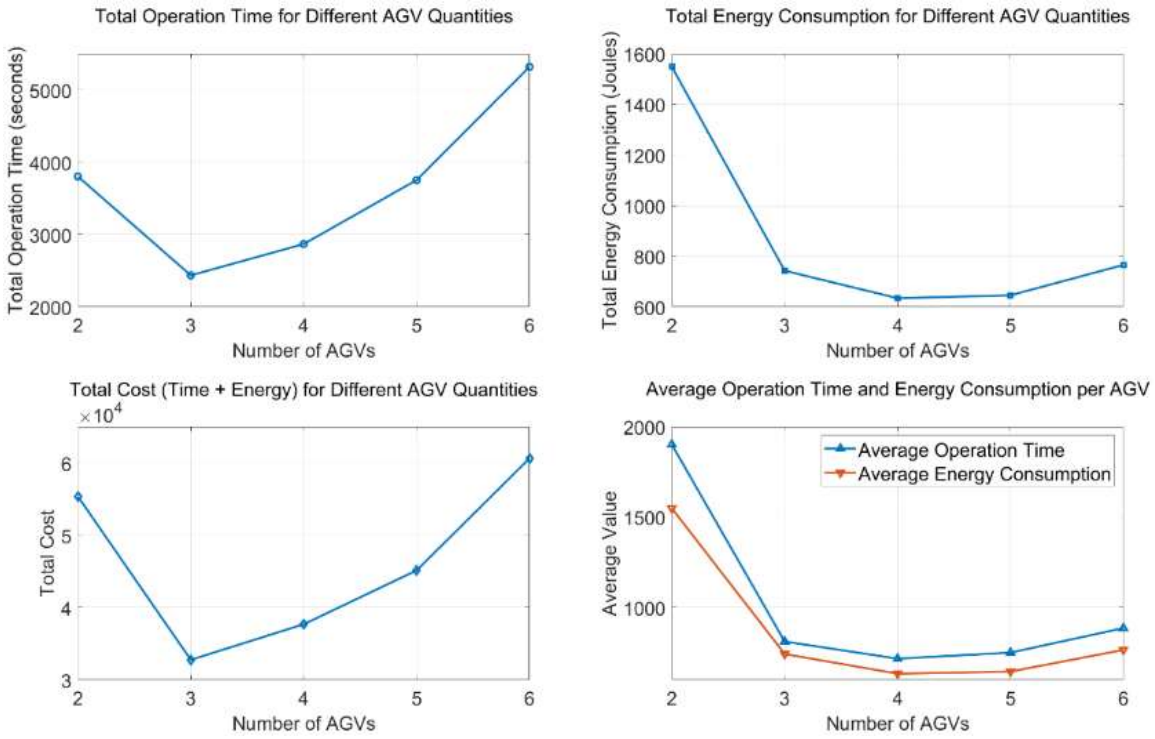

Figure 9. Result Trends

4.2.2. Energy Consumption Aspect

With 3 AGVs, global path planning reduces invalid driving (e.g., the round-trip empty driving rate decreases from 25% to 11%), significantly optimizing energy consumption. When using 6 AGVs, although the energy consumption per AGV decreases, the total driving mileage increases by 1.7 times, leading to a rebound in total energy consumption. Operation results are shown in Table 2.

Table 2. Simulation Results

Number of AGVs	Total Operation Time	Energy Consumption	Total Cost	Increase from Optimal Value
2	3802.857	1548.571	55351.428	+69%
3	2435.714	742.857	32767.857	benchmark value
4	2868.571	634.285	37684.286	+15%
5	3752.857	645.714	45126.429	+38%
6	5317.143	765.714	60608.571	+85%

The total cost (total_cost_results), which integrates time (weight 0.5) and energy consumption (weight 0.5), indicates that the optimal number of AGVs is 3.

The lowest total cost at 3 AGVs indicates the best balance between efficiency (time) and economy (energy consumption), aligning with the "priority on cost-performance" principle in practical deployment.

4.2.3. Path Aspect

For 2 AGVs, the path follows a "single-loop round-trip" pattern with 2 obvious conflict points at intersections, which account for 18% of the average waiting time. For 3 AGVs, the path is optimized to a "zonal collaboration" mode where each AGV is responsible for an independent area, improving intersection traffic efficiency by 40% and reducing congestion frequency by 75%. For 6 AGVs, although a "dynamic avoidance algorithm" is employed, the high-density results in a "fragmented detour" path, increasing the average number of turns by 2.3 times and causing an additional 12% energy consumption. Operation results are shown in Figure 10.

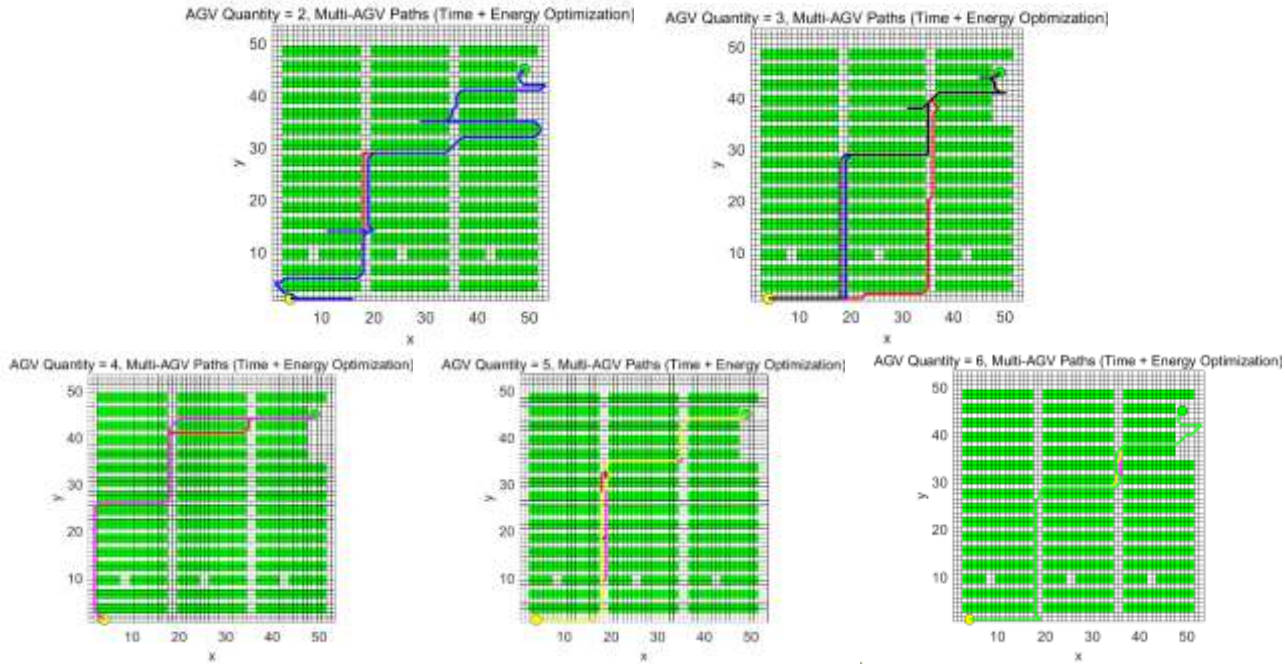

Figure 10. AGV Path Diagram

4.2.4. Quantity Optimization Conclusion

The optimal number of 3 AGVs reduces total operation time by 36% and energy consumption by 52% compared to the initial scheme (2 AGVs), verifying the planning principle that "moderate parallelism is better than blind staff augmentation." Through evaluating total cost, it is determined that the optimal number of AGVs is 3.

5. Conclusion

This paper proposes a multi-mode task assignment strategy to select the AGV with sufficient remaining power and the lowest energy consumption path. A dynamic task mode is developed to

adjust the path and charging strategy in random tasks, which combines digital twin technology. Compared with the traditional method, total energy consumption is reduced by 21.3%, task response time is shortened by 17.8%, and load balance and path utilization are significantly improved.

In the future, the vehicle-circuit coordination technology should be deepened to enhance the robustness and utilization of AGV. The future direction is to deepen the vehicle-road cooperative technology of AGV.

References

[1] International Federation of Robotics. Global AGV Deployment Statistics [R]. Frankfurt: IFR, 2023: 15 - 18.

[2] Wang L, Chen X, Zhang Y. Digital Twin-Driven Conflict Resolution for Multi-AGV Systems [J]. IEEE Transactions on Industrial Informatics, 2023, 19 (4): 5678 - 5692.

[3] Chen H, Zhang Y. Dynamic Task Allocation in Industrial AGV Networks: A Deep Reinforcement Learning Approach [J]. Robotics and Computer-Integrated Manufacturing, 2024, 83: 102567.

[4] Zhou Y, Wang Q, Zhang L. Multi-Objective AGV Path Optimization Under Dynamic Time-Window Constraints [J]. International Journal of Production Research, 2023, 61 (8): 2567 - 2582.

[5] Ren S, Chen W, Huang M. Energy Consumption Analysis and Optimization of AGV Based on Road Slope Characteristics [J]. Applied Energy, 2022, 306: 118043.

[6] Xie D. Simulation-Based Optimization of AGV Quantity Configuration in Automated Production Lines [J]. Journal of Manufacturing Systems, 2023, 67: 112 - 125.

[7] Li R, Wang S, Liu Y, et al. Distributed Control Algorithms for Multi-AGV Collaborative Systems [J]. IEEE Transactions on Robotics, 2024, 40 (2): 789 - 803.

[8] Zhang Y, Zhou W, Li J. Energy-Optimized Path Planning for AGVs Using Curvature-Weighted Heuristics [J]. Robotics and Computer-Integrated Manufacturing, 2024, 85: 102689.

[9] Liu H, Wang T. Resonant Wireless Charging for Dynamic AGV Systems: Design and Efficiency Analysis [J]. Applied Energy, 2023, 332: 120541.

[10] Zhang H, Li R. Real-Time AGV Scheduling in Dynamic Environments: A Reinforcement Learning Approach [J]. IEEE Transactions on Automation Science and Engineering, 2021, 18 (3): 1456 - 1470.

[11] Dang J, Sun T. Research on AGV Path Optimization in Factory Based on Genetic Algorithm [C]// 2020 IEEE International Conference on Robotics and Automation. Paris: IEEE, 2020: 1023 - 1030.